Oct 14th, 12:00 AM

Impact of Global Flexural Imperfections on the Cold-formed Steel Column Curve

Benjamin W. Schafer

Benjamin W. Schafer

Nineteenth International Specialty Conference on Cold-Formed Steel Structures
St. Louis, Missouri, U.S.A, October 14 & 15 2008

Impact of global flexural imperfections on the cold-formed steel column curve

Schafer, B.W.[1], Zeinoddini, V.M[2].

ABSTRACT

Due to inherent complications in manufacturing and installation global out-of-straightness imperfections in cold-formed steel columns may sometimes be greater than L/960, which is the maximum amount assumed in North American cold-formed steel design specifications. The correction that should be applied to currently used column design curves to account for imperfections larger than L/960 is unknown. To find this correction the strength of typical cold-formed steel columns with explicit imperfections is determined using a geometric and material nonlinear beam finite element solution, and a closed-formed solution. The closed-formed solution is shown to agree well with the finite element solution and accurately recreates the current design specification column curves at the L/960 imperfection level. The closed-formed solution is used as the basis for predicting reductions in the nominal column stress for columns with imperfections that are greater than L/960. The developed solution is recommended in design for those situations in which large out-of-straightness imperfections are encountered.

INTRODUCTION

Cold-formed steel columns, like all columns, are sensitive to geometric imperfections, such as out-of-straightness. Under axial load, imperfections (δ_o) lead to lateral deformations (δ) which create bending demand on the columns, known as P-δ moments. As a result of imperfections, even a column with

[1] Associate Professor, Department of Civil Engineering, Johns Hopkins University, Baltimore, MD 21218
[2] Graduate Student, Department of Civil Engineering, Johns Hopkins University, Baltimore, MD 21218

perfectly aligned axial load undergoes compression and bending. However, it is inconvenient to consider every column as a beam-column, thus the effect of P-δ moments occurring due to δ_o imperfections are empirically buried into column curves used in design.

For hot-rolled steel the AISC column curve (i.e., AISC 2005) assumes an out-of-straightness imperfection, δ_o, of L/960, where L is the column length (Galambos 1998). The column curve for cold-formed steel was determined based on comparing test data to the AISC column curve, with appropriate reductions for local buckling. This comparison lead to the adoption of the AISC column curve in cold-formed steel design (i.e., AISI-S100 2007). As a result, the maximum assumed out-of-straightness in a cold-formed steel column curve is also L/960.

Production of a cold-formed steel column involves the potential for larger out-of-straightness imperfections than a typical hot-rolled steel column. Therefore, this paper investigates the implication of considering larger δ_o imperfections in cold-formed steel and the impact of these larger δ_o imperfections on cold-formed steel column capacity and the cold-formed steel column design curve.

AISI-COFS Stud Preliminary Out-of-Straightness Study Request

In May of 2007 a task group of the American Iron and Steel Institute – Committee on Framing Standards (AISI-COFS) developed the outline for a study to assess the impact of global (sweep) imperfections on cold-formed steel columns. Essentially, the idea for their study was to model columns in MASTAN (Ziemian 2007) with explicit geometric imperfections and vary the length of columns in order to generate column capacities as a function of the size of geometric imperfection. This paper was written in response to this study, but goes beyond the specific requests of this study to explore column curve sensitivity to global imperfections using both MASTAN and a more straightforward closed-formed solution.

NUMERICALLY GENERATED COLUMN CURVE VIA MASTAN

Column strength for different imperfections

Material and geometric nonlinear MASTAN analysis (simple step using ~ 1000 steps to failure) of simply supported columns with an initial circular out-of-straightness δ_o of L/960, L/768, and L/384 was completed on a 350S162-33 (SSMA nomenclature) stud with f_y = 33ksi and KL/r_y varying from 62 to 122. The predicted column capacity from these MASTAN analyses is provided along with the AISI column curve in Figure 1. The MASTAN predicted column curves follow the same basic trend as the AISI column curve, indicating that the

analysis is capturing the basic column failure. The MASTAN analyses conducted here only include the impact of out-of-straightness on global weak-axis flexural buckling. Local buckling, torsional-flexural buckling, details of the material stress-strain curve, residual stresses, etc. are ignored.

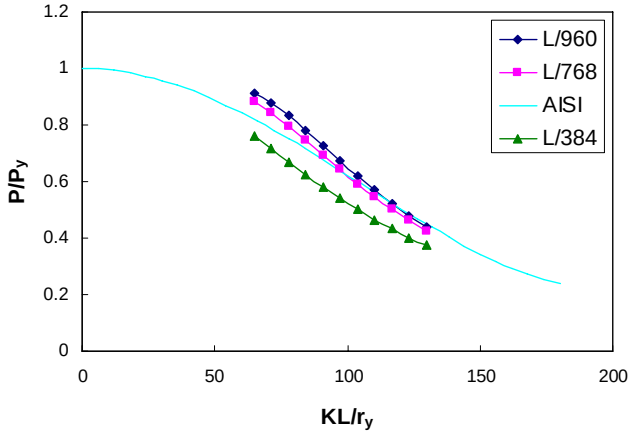

Figure 1 MASTAN predicted column curves for 350S162-33 with varying imperfection size

Influence of imperfection shape

Due to the manufacturing process a likely out-of-straightness imperfection shape for a cold-formed steel column is a constant curvature sweep in the weak-axis direction. Typical theoretical solutions employ a sinusoidal imperfection (since the solution from the differential equation for the buckling mode is itself a sinusoid). The simplest imperfection to introduce into a model is a kink, where the column is modeled as 2 straight lines with an imperfection at midspan.

The importance of imperfection shape is studied for a 350S162-33 at KL/r_y of 97 with δ_o=L/960 in Figure 2. Figure 2 demonstrates that the magnitude of the midspan deflection (δ_o) is far more important than the shape. A sinusoidal imperfection delivers slightly less P-δ moment than a constant curvature circular imperfection, but the difference is insignificant. The kink or 2-line imperfection is slightly unconservative, in that less P-δ moment is generated at a given level of P when compared with the circular or sinusoid imperfection shape.

CLOSED-FORM SOLUTION FOR COLUMN CURVE

For the simplified case of a pin-ended column in flexural buckling it is possible to develop a closed–form expression for the column capacity as a function of initial imperfection magnitude. The derivation relies on (i) providing the P-δ moment in a functional form, and (ii) providing the beam-column interaction equation (yield surface in MASTAN parlance) in a functional form. The intersection of the load, P, and moment, P-δ, with the beam-column interaction equation provides the column capacity.

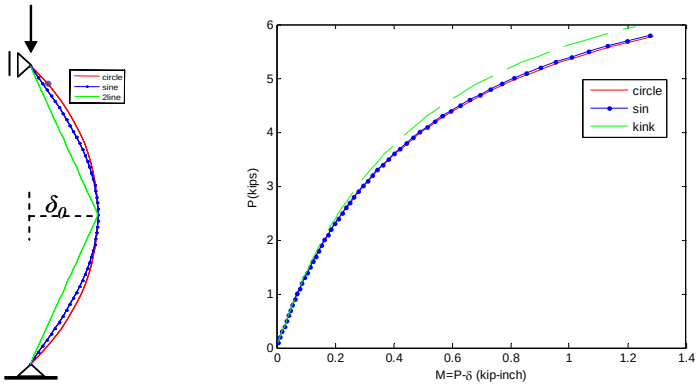

(a) imperfect shape (b) P-M response

Figure 2 P-δ response for different out-of-straightness imperfection shapes on a 350S162-33 stud with a KL/r_y of 97.2 under increasing axial load

Geometric nonlinearity

For a pin-ended column with a sinusoidal initial imperfection of midspan magnitude, δ_o, it may be shown (e.g., Chen and Lui 1987) that the midspan moment, which in the linear elastic case is simply $P\delta_o$ grows significantly as the axial load approaches the buckling load of the column. In particular, the midspan moment M may be expressed as

$$M = B_1 M_o \quad (1)$$

$$M_o = P\delta_o \quad (2)$$

$$B_1 = 1/(1-P/P_{cr}) \quad (3)$$

$$P_{cr} = \pi^2 EI_y/L^2 \quad (4)$$

Interaction equation

Column failure occurs when the P-δ moment, M, grows to the extent that the bending capacity of the column is exceeded. A linear beam-column interaction equation as used in AISI-S100 may be used for predicting when this occurs, via:

$$P/P_{no} + M/M_{no} \leq 1 \quad (5)$$

Where the equation is anchored by the assumed capacity in pure compression (P_{no}) and in pure bending (M_{no}). For the work herein:

$$P_{no} = A_g f_y = P_y \quad (6)$$

$$M_{no} = S_{effy} f_y \quad (7)$$

where the weak axis effective section modulus (S_{effy}) is determined via AISI-S100[3]. The squash load $A_g f_y$ is used instead of the effective axial load $A_{eff} f_y$ only to provide more convenient comparison between AISI and the generated closed-formed curves. (If $A_{eff} f_y$ is used for P_{no} the closed-form solution of this section is unchanged, but the AISI column curve determines A_{eff} at stress f_n, where f_n varies from f_y down to f_{cr} for global buckling as a function of the column global slenderness. To avoid calculation of A_{eff} for any global column slenderness in generation of the AISI column curve, A_{eff} is set to A_g herein.)

Column strength as a function of imperfection size

Substituting Eq. (2) and (3) into Eq. (1) and the resulting expression into Eq. (5) one finds:

$$P/P_{no} + [P\delta_o(1/(1-P/P_{cr}))]/M_{no} \leq 1 \quad (8)$$

Setting the interaction equation equal to 1.0 and solving for the axial load, P, results in a quadratic equation in terms of P. The solution to Eq. (8) provides a column capacity, P, which is a function of P_{cr}, P_{no}, M_{no}, and δ_o, where the typical column curve can be shown to be a function of only P_{cr} and P_{no}, but independent of M_{no} and δ_o. Solving Eq. (8) for P, the column capacity, results in:

$$M_{no}P^2 + (-M_{no}P_{cr} - \delta_0 P_{cr}P_{no} - P_{no}M_{no})P + P_{no}M_{no}P_{cr} = 0 \quad (9)$$

The solution to which is readily found as:

$$P = \frac{-b - \sqrt{b^2 - 4ac}}{2a} \quad (10)$$

where: $a = M_{no}$ (11)

$$b = -M_{no}P_{cr} - \delta_0 P_{cr}P_{no} - P_{no}M_{no} \quad (12)$$

$$c = P_{no}M_{no}P_{cr} \quad (13)$$

[3] AISIWIN v7.0 (Madsen 2007) was used for determining S_{effy}.

Example column curves using closed-form solution

Using Eq. (10) column curves were generated for a 362S162-68 (50 ksi) and a 800S200-97 (50 ksi) as given in Figure 3 and Figure 4. The generated column curves using the closed-formed solution agree well with the AISI column curve in trend and magnitude and also shed further light on the regimes where sensitivity to out-of-straightness imperfection are the greatest. The results confirm that the existing AISI column curve inherently assumes an imperfection in the neighborhood of L/960 and that the closed-formed solution can accurately model this effect.

The loss in column capacity for the 362S162-68 (50 ksi) and 800S200-97 (50 ksi) as δ_o increases above L/960 is shown in Figure 5 and Figure 6. The reduction in the column capacity is greatest in the low to intermediate slenderness range. If a column is slender the initial imperfection does not have a significant impact on the capacity, this is because as P approaches P_{cr} the P-δ moments quickly amplify leading to a capacity for P that asymptotes to P_{cr} for any δ_o. However, in the inelastic regime the δ_o can have a significant impact, for instance a strong reduction occurs around an unbraced length of 3 ft for the 362S162-68 and 4 ft for the 800S200-97.

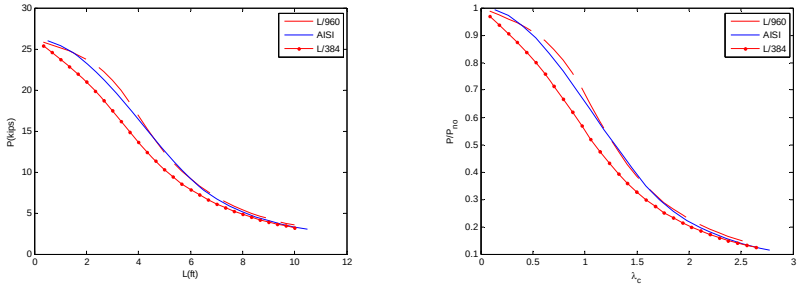

(a) L (ft) vs P (kips) (b) $\lambda_c = \sqrt{P_y / P_{cr}}$ vs. P/P_{no}

Figure 3 Predicted column curves for 362S162-68 (50 ksi) for varying imperfections

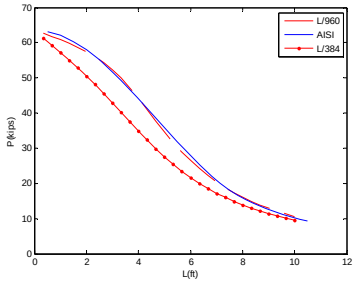

(a) L (ft) vs P (kips)

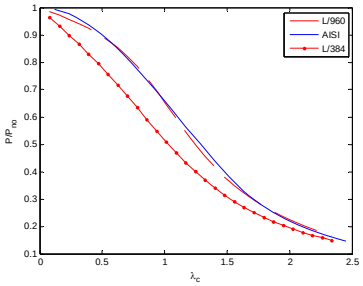

(b) $\lambda_c = \sqrt{P_y / P_{cr}}$ vs. P/Pno

Figure 4 Predicted column curves for 800S200-97 (50 ksi) for varying imperfections

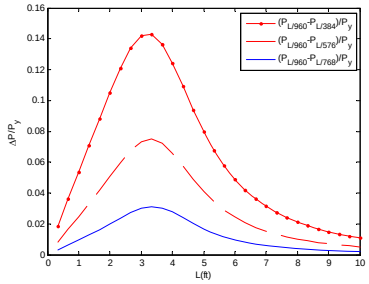

(a) L (ft) vs loss in P/P_{no}

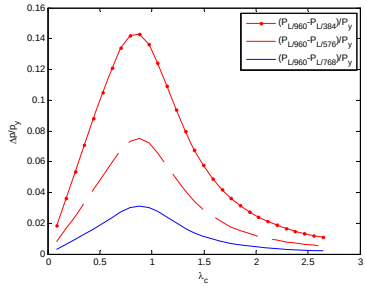

(b) $\lambda_c = \sqrt{P_y / P_{cr}}$ vs. loss in P/P_{no}

Figure 5 Predicted loss in strength for 362S162-68 (50 ksi) as imperfections increase beyond L/960

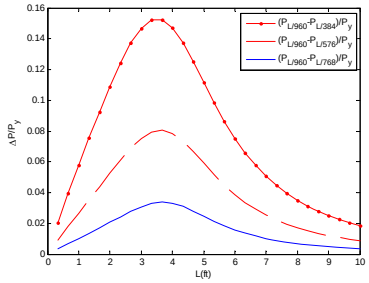

(a) L (ft) vs loss in P/P_{no}

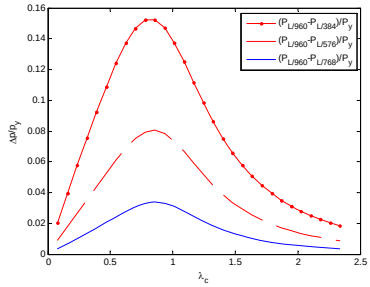

(b) $\lambda_c = \sqrt{P_y / P_{cr}}$ vs. loss in P/P_{no}

Figure 6 Predicted loss in strength for 800S200-97 (50 ksi) as imperfections increase beyond L/960

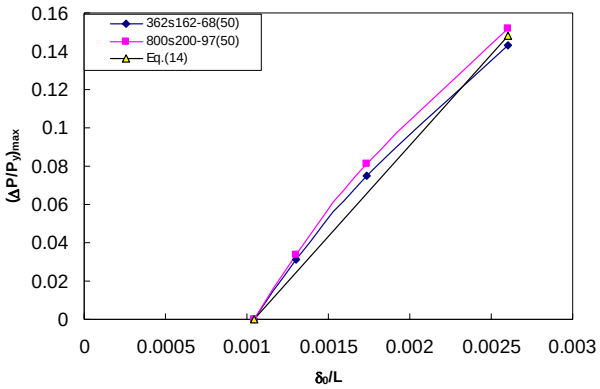

Figure 7 Maximum loss in column strength as a function of imperfection size

Column curve reductions for imperfections

The maximum reduction in the column capacity (peak error in Figure 5 and Figure 6) is plotted as a function of imperfection size in Figure 7. Interestingly, the reduction as a function of P_y is nearly the same for the 362S162-68 and the 800S200-97, which is a bit surprising given how substantially different these sections are. Taking advantage of this fact, a simple empirical relation is found for the reduced capacity:

$$(\Delta P/P_y)_{max} = 95(\delta_o/L\text{-}1/960) \text{ for } \delta_o > L/960 \tag{14}$$

Use of Eq. (14) for predicting the loss in strength due to imperfections captures only the maximum loss in strength; however this loss varies as a function of length (or equivalently λ_c) as shown in Figure 5 and Figure 6. With the peak loss known from Eq. (14) a simple empirical relation is found for the loss at all column slenderness:

$$\Delta P / P_y = \begin{cases} \dfrac{(\Delta P / P_y)_{max}}{0.85}\lambda_c & \text{if } \lambda_c \le 0.85 \\ \dfrac{(\Delta P / P_y)_{max}\, 0.85^2}{\lambda_c^2} & \text{if } \lambda_c > 0.85 \end{cases} \tag{15}$$

Comparison of Eq. (15) to the closed-form solution of Eq. (10) is provided in Figure 8. The empirical relationship of Eq. (15) provides a reasonably accurate estimation to the more involved closed-form expressions.

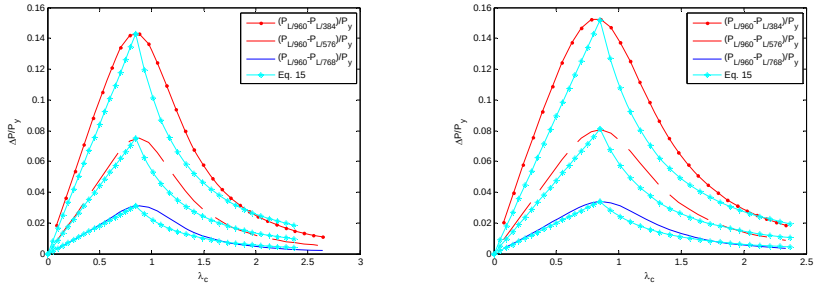

(a) $\lambda_c = \sqrt{P_y / P_{cr}}$ vs. loss in P/P_{no} for 362S162-68

(b) $\lambda_c = \sqrt{P_y / P_{cr}}$ vs. loss in P/P_{no} for 800S200-97

Figure 8 Comparison of closed-form solution (Eq. 10) with empirical expressions (Eq. 15) for predicting the loss in column capacity for imperfections beyond L/960

COMPARISON OF MASTAN AND CLOSED-FORMED SOLUTION

Geometric nonlinearity

The closed-form solution uses the B_1 multiplier (Eq. 3) to determine the P-δ moments. To demonstrate that B_1 and MASTAN provide the same solution to this geometrically nonlinear problem a 350S163-33 with δ_o=L/960 and KL/r = 64.8 and 130 was analyzed in MASTAN and compared to Eq. (3) in Figure 9. MASTAN closely tracks the theoretical solution. In this simple case, B_1 can replace the more involved geometrically nonlinear analysis completed in MASTAN as shown in Figure 9.

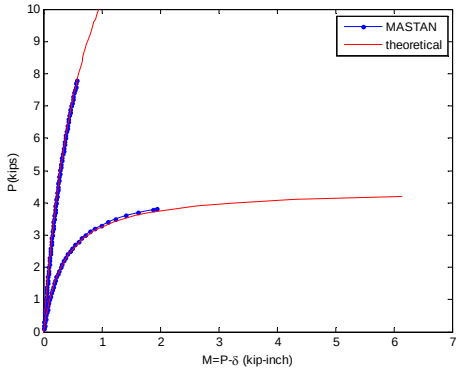

Figure 9 Prediction of P-δ moments

Yield surface

In MASTAN the failure of the column is predicted to occur when the midspan P-δ moment increases to the point it reaches the yield surface[4]. The yield surface is anchored by the assumed capacity in pure compression (P_{no}) and in pure bending (M_{no}) as discussed previously.When the P-δ moments increase to such an extent that they intersect the yield surface – at this point a plastic hinge is assumed to form in the column, and for an isolated pin-ended column, this hinge formation is equivalent to axial collapse. The normalized yield surface employed in MASTAN, along with a simple linear yield surface (as used in the closed-formed solution) is shown along with the demands from two analyses in Figure 10. The two analyses are for a 350S162-33 with δ_o=L/960, f_y=33ksi, $P_{no}=A_g f_y$, $M_{no}=S_{eff} f_y$, and KL/r_y=64.8 and 130. The axial load (P) at which the demand curves intersect the yield surface is the column capacity.

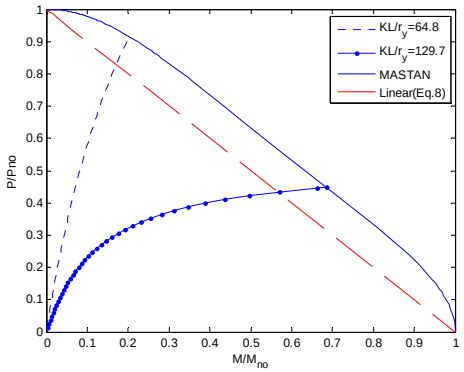

Figure 10 Comparison of yield surfaces

The MASTAN yield surface is less conservative than the simple linear yield surface (interaction equation). For low moment (little P-δ effect) the difference in axial load prediction between the two surfaces can be fairly large; however, in cases with larger P-δ moment the demand is nearly horizontal and the resulting difference in P is small. AISI-S100 conservatively assumes the linear interaction

[4] In conventional finite element analysis the yield surface is a function of stress, for concentrated plasticity beam elements typically the yield surface is integrated over the cross-section so that the surface is a function of forces and moments. The resulting yield-surface in force-moment space is essentially a beam-column interaction equation. In MASTAN the default yield surface follows the following equation: $p^2+m^2+3.5p^2m^2=1$ (Eq. 10.18 McGuire et al. 2000) and is calibrated to match a typical W-section in strong-axis bending. With appropriate changes to the compression and bending anchors this function has been shown to be a reasonable (but approximate) choice for other shapes.

equation is applicable to cold-formed steel beam-columns, and this is used in the closed-formed solution provided herein.

Column curves

The only real difference between the closed-formed solution and MASTAN is the shape of the yield surface, as described in the previous section. This difference does result in slightly different predictions for the column capacity, as shown in Figure 11 for a 350S162-33 (33ksi), δ_o=L/960.

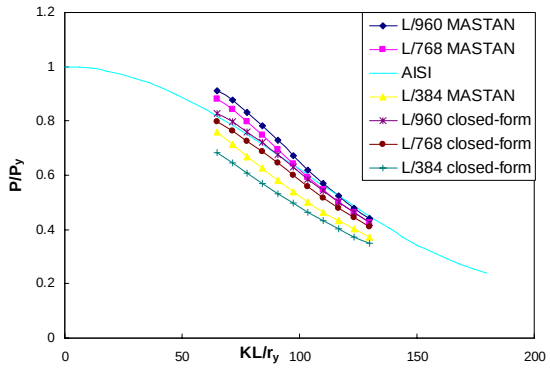

Figure 11 Comparison of MASTAN imperfect models with column curve

Imperfection sensitivity

Although the column curves from MASTAN and the closed-formed solution are slightly different (Figure 11) the relative loss in strength between the different imperfection magnitudes is essentially the same. For the same section as Figure 11 the predicted loss in strength normalized to the squash load is shown for MASTAN and the closed-formed solution in Figure 12. Use of the closed-formed solution is recommended for all cases.

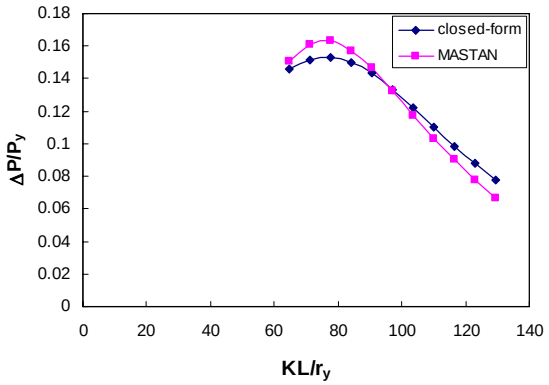

Figure 12 Comparison of predicted strength drop between L/960 and L/384 imperfections for MASTAN and closed-formed solution

DESIGN RECOMMENDATIONS

Based on the findings presented herein the following is recommended as a correction for the strength of cold-formed steel columns when imperfections are found to be greater than L/960. The nominal stress for a column is predicted from the existing AISI-S100 column curves as:

$$F_n^* = \begin{cases} 0.658^{\lambda_c^2} F_y & \text{if } \lambda_c \le 1.5 \\ \dfrac{0.877}{\lambda_c^2} F_y & \text{if } \lambda_c > 1.5 \end{cases} \tag{16}$$

where the column slenderness is defined as

$$\lambda_c = \sqrt{F_y / F_e}\ , \tag{17}$$

and where F_y is the yield stress, and F_e is the global elastic buckling stress (minimum of flexural and torsional-flexural). From Eq. (14) we may define the maximum reduction in the nominal column stress due to imperfections which are greater than L/960 as:

$$(\Delta F_n)_{max} = 95(\delta_o / L - 1/960)F_y \text{ for } \delta_o > L/960 \tag{18}$$

From Eq. (15) the reduction is known as a function of slenderness, λ_c, and may be expressed as:

$$\Delta F_n = \begin{cases} \dfrac{(\Delta F_n)_{max}}{0.85}\lambda_c & \text{if } \lambda_c \le 0.85 \\ \dfrac{(\Delta F_n)_{max}\,0.85^2}{\lambda_c^2} & \text{if } \lambda_c > 0.85 \end{cases} \tag{19}$$

where finally the nominal stress to be used in design is

$$F_n = F_n^* - \Delta F_n \tag{20}$$

If a simpler estimate of column nominal stress is needed $(\Delta F_n)_{max}$ may conservatively be used in place of ΔF_n. The preceding recommendations conservatively extend the reductions found for flexural buckling to the case of torsional-flexural buckling.

Tabulated design examples following the equations suggested above are provided for the 362S162-68 (50 ksi) and 800S20097 (50ksi) in the Appendix.

CONCLUSIONS

The strength of cold-formed steel columns is sensitive to imperfections. As axial load increases the imperfections lead to P-δ moments at midspan which eventually cause the bending capacity of the section to be exceeded and collapse to occur. It is possible to model both the increasing P-δ moment and the combination of axial load and moment that cause collapse using simple functions as is reported in the closed-formed solution herein. The presented closed-form solution agrees well with empirically derived cold-formed steel column design curves as well as advanced geometric and material beam finite element analysis solutions (MASTAN). Based on the closed-formed solution simple functions were determined for the appropriate reduction in the cold-formed steel column design strength when imperfections are greater than L/960. The reduced nominal column stress is recommended for use in design when out-of-straightness imperfections are known to be greater than L/960.

ACKNOWLEDGMENTS

This work initiated in part through conversations with Tom Trestain regarding the impact of column out-of-straightness on cold-formed studs. This material presented herein is based in part upon work supported by the National Science Foundation under Grant No. 0528318. Any opinions, findings, and conclusions or recommendations expressed in this material are those of the author(s) and do not necessarily reflect the views of the National Science Foundation.

REFERENCES

AISC (2005). Specification for Structural Steel Buildings. American Institute of Steel Construction, Chicago, IL. ANSI/ASIC 360-05

AISI (2007). North American Specification for the Design of Cold-Formed Steel Structures. American Iron and Steel Institute, Washington, D.C., AISI-S100.

Chen, W.F., Lui, E.M. (2007). Structural Stability: Theory and Implementation. Prentice-Hall.

Galambos, T. (1998) "Guide to Stability Design Criteria for Metal Structures". 5th ed., Wiley, New York, NY, 815-822.

Madsen (2007) AISIWIN, v7.0, Devco Software, http://www.devcosoftware.com/aisiwin.html last visited 11 July 2007.

McGuire, W., Gallagher, R.H., Ziemian, R.D. (2000). Matrix Structural Analysis. 2nd Edition. Wiley.

Ziemian (2007) MASTAN, v3.0, www.mastan2.com last visited 11 July 2007.

APPENDIX: TABULATED COLUMN DESIGN EXAMPLE

Example column calculations for imperfection sensitivity
BWS
August 2007

362S162-68 (50 ksi)

E	29500	ksi
$I_{yygross}$	0.1858	in^4
A_{gross}	0.5237	in^2
F_y	50	ksi

This example illustrates the loss in axial capacity for a 362S162-68 (50ksi) with an out-of-straightness of L/384 as the unbraced length is increased from 3 ft up to 8 ft. The nominal axial capacity is calculated by (1) ignoring the out-of-straightness using AISI 2007 and reported as P_n* below, (2) using the recommended expressions in Section "design recommendations" of the paper, reported as P_n below, and (3) using the original derived strength reductions from Section "closed form solution for column curve" of the paper, Pn2.

	AISI 2007 (Eq. 17) (Eq. 16)					Design Method - stress based reduction - Section 6 of Paper (Eq. 18) (Eq. 19) (Eq. 20)								Strength reduction - Section 4 (Eq. 14) (Eq. 15)			
KL	F_e	λ_c	F_n*	$A_e(F_n$*)	P_n*	δ_o (L/384)	$(\Delta F_n)_{max}$	ΔF_n	F_n	$A_e(F_n)$	P_n	P_n*-P_n	$(P_n$*-$P_n)/P_n$*	$(\Delta P)_{max}$	ΔP	P_{n2}	$(P_n$*-$P_{n2})/P_n$*
(ft)	(ksi)		(ksi)	(in^2)	(kip)	(in)	(ksi)	(ksi)	(ksi)	(in^2)	(kip)	(kip)		(kip)		(kip)	
3	79.70	0.79	38.45	0.491	18.87	0.094	7.42	6.92	31.54	0.504	15.88	2.98	16%	3.89	3.62	15.25	19%
4	44.83	1.06	31.35	0.504	15.80	0.125	7.42	4.81	26.54	0.515	13.66	2.14	14%	3.89	2.52	13.29	16%
5	28.69	1.32	24.11	0.521	12.56	0.156	7.42	3.08	21.03	0.524	11.01	1.54	12%	3.89	1.61	10.95	13%
8	11.21	2.11	9.83	0.522	5.13	0.250	7.42	1.20	8.63	0.524	4.52	0.61	12%	3.89	0.63	4.50	12%

800S200-97 (50 ksi)

E	29500	ksi
$I_{yygross}$	0.576	in^4
A_{gross}	1.2706	in^2
F_y	50	ksi

This example illustrates the loss in axial capacity for an 800S200-97 (50ksi) with an out-of-straightness of L/384 as the unbraced length is increased from 3 ft up to 8 ft. The nominal axial capacity is calculated by (1) ignoring the out-of-straightness using AISI 2007 and reported as P_n* below, (2) using the recommended expressions in Section 6 of the paper, reported as P_n below, and (3) using the originall derived strength reductions from Section 4 of the paper, P_{n2}.

	AISI 2007 (Eq. 17) (Eq. 16)					Design Method - stress based reduction - Section 6 (Eq. 18) (Eq. 19) (Eq. 20)								Strength reduction - Section 4 (Eq. 14) (Eq. 15)			
KL	F_e	λ_c	F_n*	$A_e(F_n$*)	P_n*	δ_o (L/384)	$(\Delta F_n)_{max}$	ΔF_n	F_n	$A_e(F_n)$	P_n	P_n*-P_n	$(P_n$*-$P_n)/P_n$*	$(\Delta P)_{max}$	ΔP	P_{n2}	$(P_n$*-$P_{n2})/P_n$*
(ft)	(ksi)		(ksi)	(in^2)	(kip)	(in)	(ksi)	(ksi)	(ksi)	(in^2)	(kip)	(kip)		(kip)		(kip)	
3	101.84	0.70	40.71	0.957	38.96	0.094	7.42	6.12	34.59	0.988	34.18	4.78	12%	9.43	7.77	31.19	20%
4	57.29	0.93	34.70	0.987	34.25	0.125	7.42	6.14	28.56	1.027	29.32	4.94	14%	9.43	7.81	26.45	23%
5	36.66	1.17	28.25	1.027	29.03	0.156	7.42	3.93	24.32	1.058	25.73	3.30	11%	9.43	5.00	24.03	17%
8	14.32	1.87	12.56	1.200	15.07	0.250	7.42	1.54	11.02	1.225	13.50	1.56	10%	9.43	1.95	13.11	13%